chemistry

MDPI

Article

Substrate–Solvent Crosstalk—Effects on Reaction Kinetics and Product Selectivity in Olefin Oxidation Catalysis

Rita N. Sales [1], Samantha K. Callear [2], Pedro D. Vaz [3,4,*] and Carla D. Nunes [1,*]

[1] Centro de Química Estrutural, Faculdade de Ciências da Universidade de Lisboa, 1749-016 Lisboa, Portugal; ritansales@gmail.com
[2] ISIS Neutron & Muon Source, Rutherford Appleton Laboratory, Chilton, Didcot, Oxfordshire OX11 0QX, UK; sam.k.callear@gmail.com
[3] CICECO—Aveiro Institute of Materials, Department of Chemistry, University of Aveiro, 3810-193 Aveiro, Portugal
[4] Champalimaud Foundation, Champalimaud Centre for the Unknown, 1400-038 Lisboa, Portugal
* Correspondence: pedro.vaz@fundacaochampalimaud.pt (P.D.V.); cmnunes@ciencias.ulisboa.pt (C.D.N.); Tel.: +351-210-480-200 (P.D.V.); +351-217-500-876 (C.D.N.)

Abstract: In this work, we explored how solvents can affect olefin oxidation reactions catalyzed by MCM-bpy-Mo catalysts and whether their control can be made with those players. The results of this study demonstrated that polar and apolar aprotic solvents modulated the reactions in different ways. Experimental data showed that acetonitrile (aprotic polar) could largely hinder the reaction rate, whereas toluene (aprotic apolar) did not. In both cases, product selectivity at isoconversion was not affected. Further insights were obtained by means of neutron diffraction experiments, which confirmed the kinetic data and allowed for the proposal of a model based on substrate–solvent crosstalk by means of hydrogen bonding. In addition, the model was also validated in the ring-opening reaction (overoxidation) of styrene oxide to benzaldehyde, which progressed when toluene was the solvent (reaching 31% styrene oxide conversion) but was strongly hindered when acetonitrile was used instead (reaching only 7% conversion) due to the establishment of H-bonds in the latter. Although this model was confirmed and validated for olefin oxidation reactions, it can be envisaged that it may also be applied to other catalytic reaction systems where reaction control is critical, thereby widening its use.

Keywords: oxidation catalysis; neutron diffraction; molybdenum; mesoporous materials; hydrogen bonds

Citation: Sales, R.N.; Callear, S.K.; Vaz, P.D.; Nunes, C.D. Substrate–Solvent Crosstalk—Effects on Reaction Kinetics and Product Selectivity in Olefin Oxidation Catalysis. *Chemistry* **2021**, *3*, 753–764. https://doi.org/10.3390/chemistry3030054

Academic Editor: José Antonio Odriozola

Received: 18 June 2021
Accepted: 16 July 2021
Published: 19 July 2021

1. Introduction

Developing selective reactions is an everyday struggle that mankind faces in order to replicate nature's work, which is remarkable at all levels. Mankind is continuously attempting to mimic something that has already had millions of years of perfection, and, therefore, an enormous amount of effort is required to achieve this.

In the case of oxidation reactions, the quest for selective processes poses an everyday challenge to both academia and industry [1–7]. To achieve the goal of developing such processes, catalysts have been produced to address the need for operating chemical transformations in an efficient and selective way. This has driven a considerable amount of research to focus on the numerous different and specific oxidation reactions, provided by the plethora of functional groups requiring oxidation, that are needed for the assessment of added-value products [8–10]. Focusing on obtaining, ideally, a single product, control of the chemical process is critical to achieving this goal, which implies that several parameters need to be identified in order to determine how to control it [4]. In the simplest cases, this can be carried out based on the kinetics of the reaction. However, this is rare, and, as such, catalysis is detrimental to progress of such a quest, sometimes tuning selectivity at the cost

of activity. This becomes even more pertinent given the sustainability goals that must be met according to commitments by several stakeholders [3,5,7].

Research into catalytic process optimization covers catalyst development ranging from a selection of several transitions metals (mostly) and their ability to work under a selection of homogeneous or heterogeneous versions with a wide range of supporting materials available [11–13]. Beyond that, research also devotes effort to determining the most suitable oxygen source (ideally dioxygen, but also organic peroxides or hydrogen peroxide), physical conditions (pressure and temperature), and the solvent [14–17]. Solvent choice is usually screened in terms of striking a balance between activity and selectivity, with the ultimate choice being made, eventually, from a sustainability point of view [18,19]. Across research on the development of efficient systems for the catalytic oxidation of olefins (Scheme 1 showing possible oxidation products), several physical parameters are usually tuned. Nevertheless, through the course of past reports, we noticed that the reaction kinetics on substrate conversion would be drastically affected by changing the solvent.

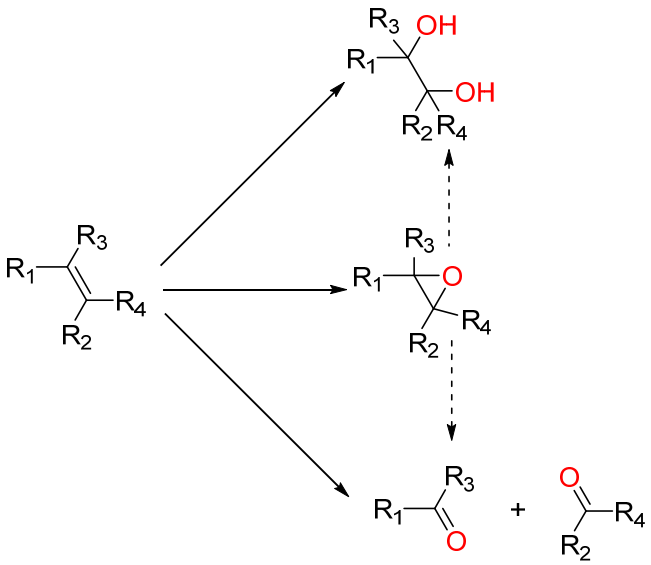

Scheme 1. Possible products in olefin oxidation reactions.

Despite that, little attention has been devoted to assessing what specific phenomena rule the differences observed in a given process when the solvent is changed. For instance, some reports on the catalytic oxidation of styrene showed that authors screened a set of solvents and made their choices depending on the best one to achieve the highest conversion, selectivity or both [20–27].

However, assessment of the effects of solvent was conducted on the basis of the nature of the solvent, i.e., protic/aprotic or polar/apolar without further in-depth analysis [28–31]. Previous reports found in the literature have described several levels of solvent effects depending on the systems studied. For instance, Zhenyan reported that the solvent drastically affected the performance of a catalytic styrene oxidation system [28]. The authors reported that the use of polar solvents with protic ones largely hindering the reaction, mostly in terms of substrate conversion. Given that protic solvents are prone and very likely to establish hydrogen bonds, this could be the reason for the observed hinderance effect. Further insights of solvent effects influencing catalytic oxidation reactions in terms of both substrate conversion and product selectivity modulation have been addressed, from the pioneering work of Corma in 1996 [32] to more recent studies [33–35]. In all of these studies, the authors attempted to provide evidence of solvent influence as an explanation for the observed effects.

Further insights into the local structure and effects of solvents at the molecular level remain scarce and are urgently needed for further contributions to the development of more

sustainable processes. Recently, a few reports addressed the influence of liquid solvents on the activity of several catalytic systems [36–38]. For instance, Emenike described how different solvents can modulate the existence of C–H···π interactions between solvents and solutes with implications on the conformational behavior of the latter [36]. In another study using total neutron scattering, the authors assessed the structure of a series of aromatic organics with an increasing degree of unsaturation at the side chain (ethyl benzene, styrene, and phenylacetylene) [39]. In that study, by examining the solvation shells, the authors found that unsaturation did not have much influence on the existence of intermolecular interactions with a preference for a chain–chain vicinity.

In this work, we describe solvent effects observed in oxidation catalysis and how they influence both substrate conversion and, in some cases, product selectivity. Specifically, experimental evidence on how the solvent interferes with the catalytic system is provided. Data on the feasibility of the proposed model that are supported by experimental and computational data are also discussed.

2. Experimental Procedures

2.1. General

All reagents were purchased from Aldrich (St. Louis, MO, USA) and used as received.

FTIR spectra were measured with a Nicolet Nexus 6700 FTIR spectrometer (Waltham, MA, USA) using a Diffuse Reflectance accessory. All FTIR spectra were measured in the 400–4000 cm^{-1} range and using 4 cm^{-1} resolution. Powder XRD measurements were taken on a Philips Analytical PW 3050/60 X'Pert PRO (theta/2 theta) (Almelo, The Netherlands) equipped with an X'Celerator detector and with automatic data acquisition (X'Pert Data Collector (v2.0b) software), using monochromatized Cu-Kα radiation as the incident beam, 40 kV–30 mA. Microanalyses were performed at the University of Vigo. The oxidation reactions described in this study were catalyzed by an Mo organometallic complex immobilized inside the pores of MCM-41 by means of a tethered bipyridine ligand. This catalyst, referred to as MCM-bpy-Mo, was reported earlier [26,40], and its synthesis is described in the SI material. Furthermore, for the validation of the solvent effects described here, one batch of MCM-41 was also synthesized and then split into two sub-batches differing in the protocol for template removal—one sub-batch was calcined, being referred to as MCM_C, while the other was subjected to a template removal procedure by refluxing it with methanol acidified with HCl, and this one is referred to as MCM_{AW}. This rendered a set of MCM with regular surface silanol groups (MCM_C), while the remaining (MCM_{AW}) had Brønsted acid silanol groups. Details regarding the synthesis procedures can also be found in the SI material. Table S1 shows isotope substitution model in neutron experiments. Characterization of MCM materials (Figure S1) was found in agreement with published data.

All catalytic reactions were conducted in a Carousel 12 Plus Reaction Station from Radleys (Shire Hill, Essex, UK), providing both temperature and atmosphere control. All reactions were monitored (substrate conversion and product yield) by sampling at regular time intervals and analyzed using a Shimadzu QP-2010 Plus GC-MS system (Kyoto, Japan).

2.2. General Procedure for Catalytic Epoxidation of Olefins

The olefin substrates (1.6 mmol)—*cis*-cyclooctene, styrene, *trans*-2-hexen-1-ol, and *R*-(+)-limonene—were mixed with dibutylether (1.6 mmol, internal standard) and 582 μL (200 mol %) of *tert*-butyl hydroperoxide (5.5 M solution in decane; tbhp) followed by addition of the solvent (acetonitrile or toluene) and MCM-bpy-Mo catalyst (3 mol %) at 353 K.

2.3. General Procedure for the Metal-Free Oxidation of Styrene Oxide to Benzaldehyde

This procedure was very similar to the previous one. Styrene oxide (1.6 mmol) was mixed with dibutylether (1.6 mmol) (internal standard) and 582 μL (200 mol %) of *tert*-butyl hydroperoxide (5.5 M solution in decane; tbhp) followed by addition of the solvent

(acetonitrile or toluene). Then, the MCM-41 catalyst (either MCM_C or MCM_{AW}, 50 mg) was added to this mixture. The magnetically stirred mixture was heated to 353 K and maintained for 24 h.

3. Results and Discussion

3.1. Solvent Effects on the Catalytic Oxidation of Olefins

In this study we addressed how solvents—acetonitrile (polar aprotic) and toluene (apolar aprotic)—interfered in the catalytic oxidation of a set of olefins. This was evidenced for the oxidation of *cis*-cyclooctene, styrene, *R*-(+)-limonene, and *trans*-hex-2-en-1-ol in the presence of the MCM-bpy-Mo catalyst using *tert*-butylhydroperoxide (tbhp) as an oxygen source (see Table S2 and Figure S2 in SI material for full results).

As can be seen from Figure 1, data from conversion of the different substrates catalyzed by the above-mentioned system showed that the reaction rates were found to be dramatically dependent on the solvent under strictly similar conditions.

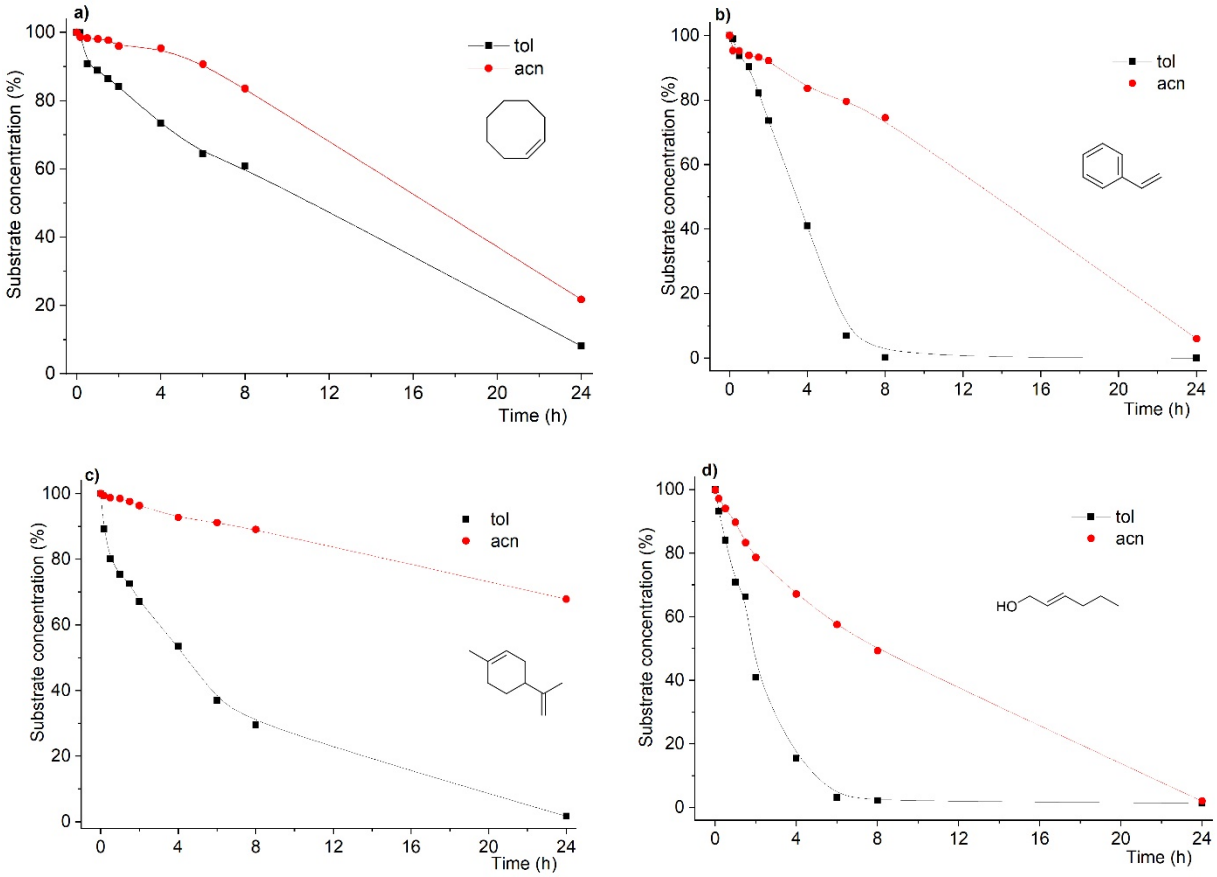

Figure 1. Kinetic profiles of substrate conversion for oxidation reactions of *cis*-cyclooctene (**a**), styrene (**b**), *R*-(+)-limonene (**c**) and *trans*-hex-2-en-1-ol (**d**) in toluene and acetonitrile. Reactions were carried out using substrate:oxidant:catalyst mol % ratio of 100:200:3 using acetonitrile or toluene as solvent and at 353 K.

Still, another feature arises from the data in Figure 1. Not only were the reaction rates affected by the solvent change, but the final conversion after 24 h was also found to follow the same dependence. As such, for most of the substrates, when acetonitrile was used as solvent, with the exception of the *trans*-hex-2-en-1-ol substrate, we found that the final conversions were lower, in some cases drastically, as in the case of *R*-(+)-limonene.

In the case of styrene (Figure 1b), the main desired product is styrene oxide. However, formation of benzaldehyde is commonly observed and often as major product. This has already been addressed by us when using MCM-based catalysts, which, due to specific surface species, are responsible for conversion of styrene into benzaldehyde [26,40]. In

the results obtained in this study using the MCM-bpy-Mo catalyst, the product yield was found to be dependent on the solvent used. In fact, when the solvent was toluene, styrene oxidation yielded benzaldehyde with 75% yield (styrene oxide with 25% yield) at 100% substrate conversion after a 24 h reaction time. On the other hand, when the reaction was conducted in acetonitrile, the product yield considerably changed: 48% for benzaldehyde and 46% for styrene oxide were obtained at 94% substrate conversion after a 24 h reaction time. This is further addressed later in this study to demonstrate that the right choice of solvent could protect styrene oxide from overoxidation.

Concerning product yield (and inherently their selectivity) in the oxidation of *R*-(+)-limonene, we also found that virtually no changes were observed at isoconversion (i.e., conversion at similar values but obtained at different reaction times) when the solvent changed. This is most evident in Figure 2, showing the reaction profile (substrate conversion and product yield) for *R*-(+)-limonene oxidation. As can be seen, at the same conversion level (ca. 34%), the product yield distribution is identical for both solvents. The striking difference, as previously mentioned, is that the 34% conversion was obtained after 24 h in acetonitrile but after only 2 h in toluene.

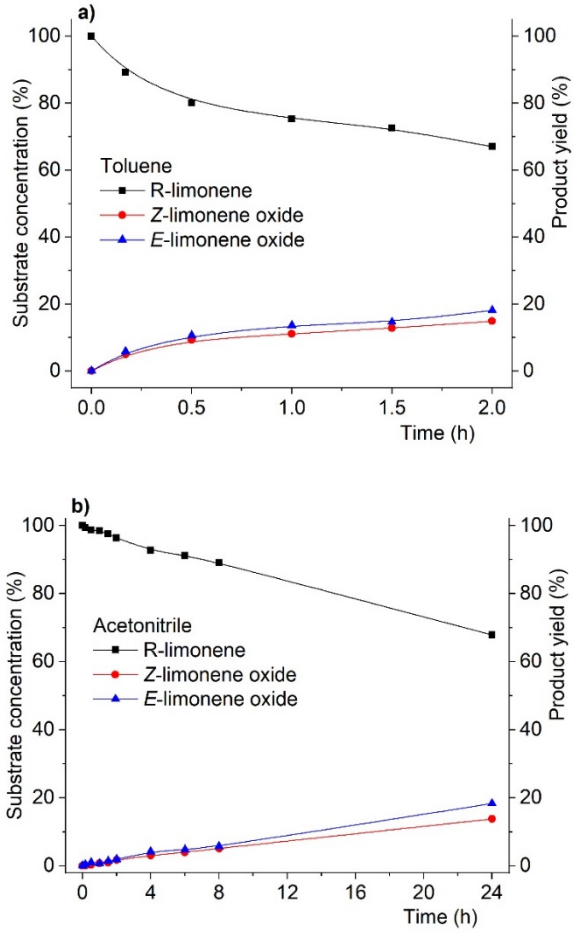

Figure 2. Reaction profiles for *R*-(+)-limonene oxidation catalyzed by MCM-bpy-Mo catalyst in toluene (**a**) and acetonitrile (**b**) at substrate isoconversion. Reactions were carried out using substrate:oxidant:catalyst mol % ratio of 100:200:3 using acetonitrile or toluene as solvent and at 3535 K.

As shown in Figure 2, these results showed that changing the solvent did not affect both product yield and the product diastereoselectivity ratio at isoconversion. In addition, these data also reveal that the solvent seems to solely influence the reaction kinetics without promoting any apparent deeper interference in the mechanism of the catalytic reaction.

Based on these results, it could be assumed that the possibility for the existence of specific solvent–substrate (or reactant) interactions, such as hydrogen bonding, could be rationalized with acetonitrile but less so with toluene [41–43].

Based on recent reports assessing the structure of liquids by means of neutron scattering techniques [39,44], in this work, we conducted an experiment to assess the local structure of styrene and the solvents mentioned above (acetonitrile and toluene) under the same *in operando* catalysis conditions. Styrene was chosen given that it is readily available as a deuterated isotopomer, which is a requirement for such experiments.

According to Figure 3, the neutron diffraction experiment demonstrated that there are differences correlated with the intermolecular interactions between styrene and the solvents (acetonitrile and toluene). In particular, the EPSR model revealed the existence of H-bonds when acetonitrile was present, whereas these were absent when toluene was used instead. This is evidenced in Figure 3a by the $H_{CH2}\cdots N{\equiv}C$ and $H_{ring}\cdots N{\equiv}C$ curves, which show a more defined peak than those in Figure 3b for the curves representing the $H_{CH2}\cdots C_{ring}$ and $H_{ring}\cdots C_{ring}$ interactions. The reason supporting the fainter peak profile in the latter is indicative of the existence of weaker intermolecular interactions. In fact, this is expected since in the styrene–toluene system (Figure 3b), intermolecular interactions are mostly C–H$\cdots\pi$, whereas in the styrene–acetonitrile system (Figure 3a), the interactions are mostly C–H$\cdots$N, which are stronger yielding; therefore, a higher degree of organization of the mixture as observed. This is verified in Figure 3a, where the $H_{CH2}\cdots N{\equiv}C$ curve clearly shows the existence of H-bonding between the acetonitrile N-atom and H-atoms in the vinyl group of styrene at lower interaction distances than those found for the H-atoms from the vinyl group and toluene. In addition, the $C_{CH2}\cdots N{\equiv}C$ curve also displays a very defined peak at 3.6–3.8 Å, confirming the existence of specific geometries most probably interacting by means of hydrogen bonds. These results provide clear and strong evidence that the existence of specific interactions between solvent and substrate is likely to be responsible for the observed kinetic effects and substrate conversion levels.

3.2. Solvent Effects on Conversion of Styrene Oxide—Model Validation

As previously mentioned earlier in this study, styrene oxidation represents somewhat of an issue in regard to product yield (and subsequently selectivity) in the presence of MCM-41-based catalysts [26,40,45]. In those works, the products were always styrene epoxide and benzaldehyde, the latter being formed either directly or by overoxidation of the former [46], with their relative selectivity presenting different results depending on the used catalyst. We recently postulated a mechanism that would be responsible for the conversion of styrene oxide into benzaldehyde and formaldehyde [26,40]. This mechanism relies on a side reaction at the MCM surface, which is rich in silanol groups, without the need for a metal catalyst; therefore, it carries out a metal-free process, as shown in Scheme 2.

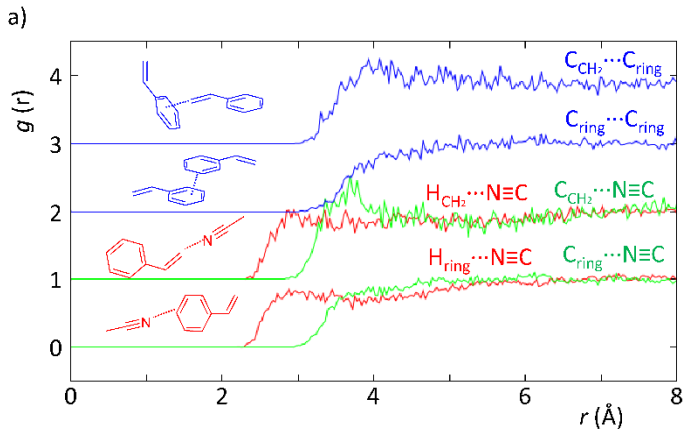

Figure 3. *Cont.*

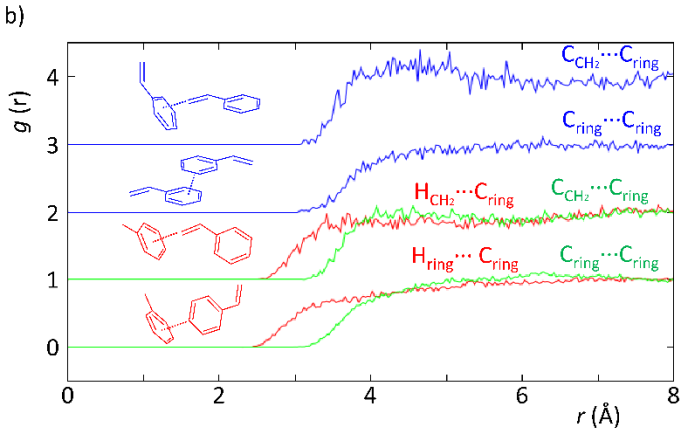

Figure 3. Partial radial distribution functions from EPSR simulation of experimental data obtained with SANDALS data from experiment RB1600022 on the styrene–acetonitrile (**a**) and styrene–toluene (**b**) systems replicating the ratios used in a catalytic experiment.

According to Scheme 2, styrene oxide binds to a Brønsted acid-site in the first step. Afterwards, the Cl^- abstracts an H-atom from tbhp, which will then attack the activated epoxide leading to the opening of the oxirane ring. Concomitantly, this also releases the HCl molecule. The intermediary formed will then decompose yielding benzaldehyde, formaldehyde and *t*-butanol. The previously released HCl molecule binds to the surface silanol regenerating the Brønsted acid-site and closing the cycle.

This proposal lacked confirmation so far. In this way, we used the specific solvent effects concept to test and validate this mechanistic proposal on the conversion of styrene epoxide into benzaldehyde [26,40], while at the same time provided insight about the active role of solvents.

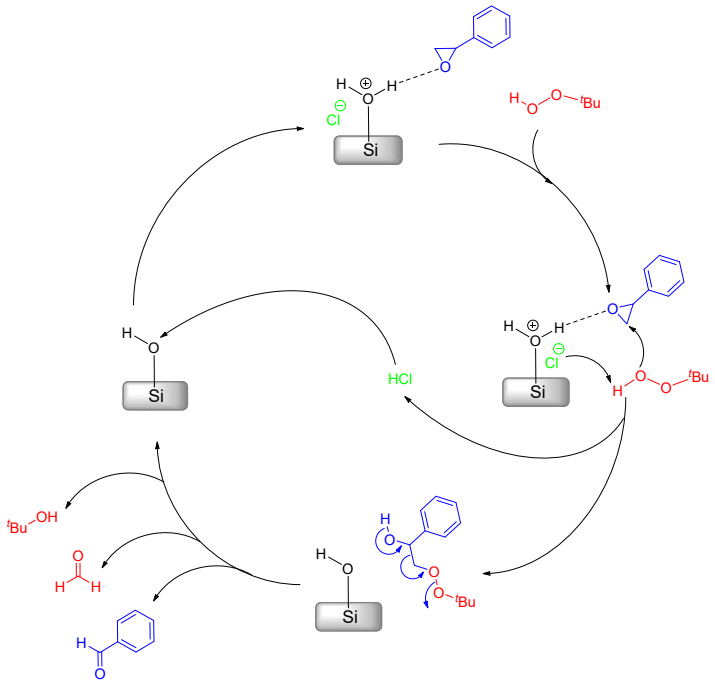

Scheme 2. Mechanistic proposal for the catalytic benzaldehyde formation from styrene oxide catalyzed by acid sites at the surface of MCM-41.

The mechanism also provided insight into the active role of solvents. We used the set of two MCM-41-related materials, MCM_C and MCM_{AW}, differing in template extraction method (see Experimental Section for details). These MCM materials, as pictured in

Scheme 3, had their surface with regular silanol groups (MCM_C) and with Brønsted acid silanol groups (MCM_{AW}) required for assistance in the postulated ring-opening process (Scheme 2) [23,39].

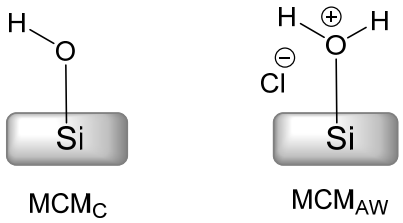

Scheme 3. Silanol species at the surface of calcined (MCM_C) and acid-washed (MCM_{AW}) MCM-41 material.

As such, starting from styrene epoxide we tested both MCM materials the reaction in toluene at 353 K was examined for 24 h (with tbhp) to confirm whether benzaldehyde could be obtained in the presence of any of the solids (MCM_C and MCM_{AW}). The results showed that benzaldehyde could not be obtained in the presence of MCM_C, but when using MCM_{AW}, the reaction proceeded normally with benzaldehyde being detected, as shown in Figure 4.

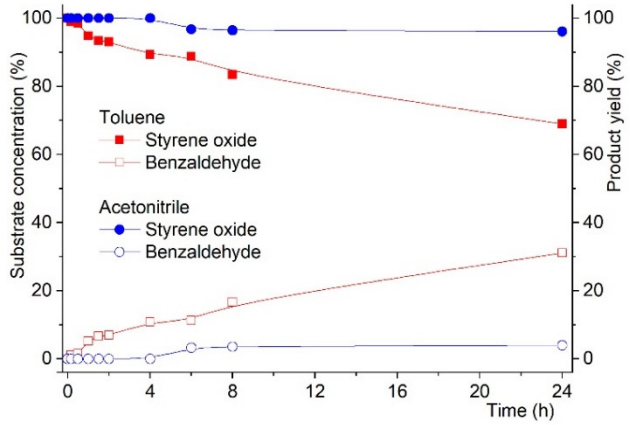

Figure 4. Reaction kinetics for the oxidation of styrene oxide to benzaldehyde in the presence of MCM_{AW}. Reactions were carried out using substrate:oxidant mol % ratio of 100:200 with 50 mg of catalyst using acetonitrile or toluene as solvent and at 3535 K.

In the case of the reaction carried out in the presence of MCM_C, styrene oxide conversion was found to be 2% when the solvent was toluene, but when the reaction was conducted in acetonitrile, no reaction was observed (0% styrene oxide conversion).

On the other hand, when the catalyst was MCM_{AW}, strikingly different results were obtained. As shown in Figure 4, styrene oxide conversion into benzaldehyde was observed to reach 31% after 24 h reaction when using toluene as solvent. Changing the solvent to acetonitrile implied a drastic change, as only 7% of styrene oxide conversion to benzaldehyde as compared to the same reaction in toluene.

The first outcome was that this showed that the presence of surface silanol groups with the acid moieties, as postulated in Scheme 2, was needed for the reaction to take place. The second outcome was that we could also demonstrate that the solvent could actively influence the reaction kinetics by establishment of specific intermolecular interactions (e.g., H-bonds), as discussed earlier in this study and confirmed by neutron diffraction experiments. In fact, the presence of acetonitrile seems to compete with the activated surface silanol groups and, thus, hinders the reaction. On the other hand, in the case of toluene, this effect did not occur to the same extent, and competition with silanol groups was not strong enough to hinder the reaction. This concept must be postulated within the

framework of the existence of specific intermolecular interactions—C–H···N and C–H···π—as discussed earlier in this study, where their existence interferes in the reaction rate by interaction with the substrate.

The above assumptions were evaluated for feasibility under the framework of DFT calculations to assess possible structures of styrene oxide with solvent molecules. As can be seen in Figure 5, the optimized structures of styrene oxide with solvent molecules (acetonitrile or toluene) display the presence of specific interactions through H-bonds. In the case of toluene, the CH_2 group in styrene oxide can interact with toluene through C–H···π bonds, whereas in the case of acetonitrile, the interaction takes place by means of C–H···N bonds.

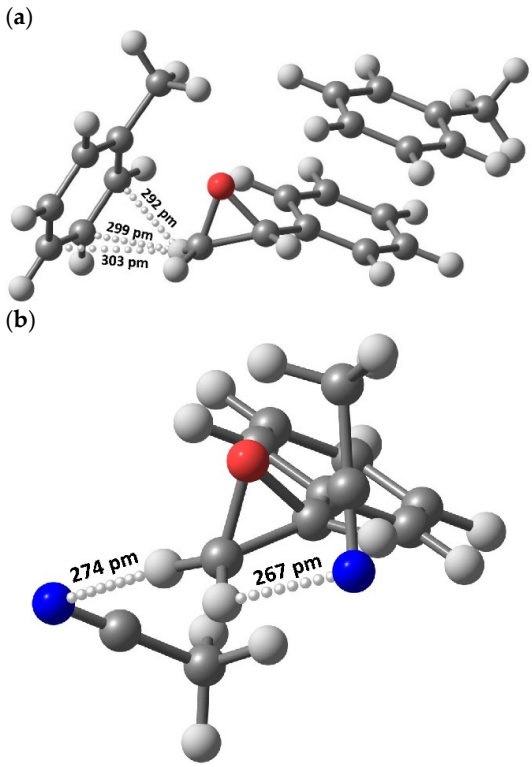

Figure 5. Optimized geometries using a DFT method showing H-bonding interactions between styrene oxide and toluene (C–H···π, (**a**)) or acetonitrile (C–H···N, (**b**)).

DFT results showed that the interaction distance is shorter for the latter—270 pm on average—compared to that in the former—298 pm, rendering a stronger bonding energy for the C–H···N interactions. These findings were corroborated by NBO topological analyses, where the Wiberg bond orders were 0.009 and 0.002 for the C–H···N and C–H···π bonds, respectively. In addition, according to Figure 5a, the represented optimized geometry shows a free unbonded H-atom in the oxirane ring, which may also be responsible for the reactivity demonstrated by this system compared with the geometry found for the acetonitrile version (Figure 5b) where both H-atoms are bonded and unavailable for reaction to benzaldehyde (Scheme 2).

Although the neutron experiments were focused on styrene, these experimental results were obtained for styrene oxide, which is a related substrate. The fact that these data agree with the results from the neutron diffraction discussed earlier in this work for the interactions between styrene and the same solvents thus validates the model in which those solvents play a direct role in the catalytic reaction.

Moreover, the findings from the DFT calculations and those obtained experimentally from the neutron diffraction experiment are coherent and support previously postulated mechanistic proposals [26,40]. In our previous mechanistic proposal for the conversion of styrene epoxide to benzaldehyde, it was proposed that the route would occur through an

H-bond assisted path. The neutron diffraction data now show that in the case of acetonitrile, where much less conversion of styrene epoxide (less benzaldehyde yield) was observed, there are explicit H-bonds. In this way, such a structure will compete with the H-bond-assisted mechanism (Scheme 2), resulting in lower performance of the catalytic system. These data agree with experimental kinetic data, as shown above in Figure 4. Furthermore, these findings are in agreement with literature data, where intermolecular interactions were described to play a non-innocent role in the structure of liquids and in styrene in particular [39].

The above results presented and discussed herein demonstrate that for the case of styrene oxidation (and styrene oxide overoxidation), reaction control can be achieved by the choice of a suitable solvent.

Styrene oxidation leading to the corresponding epoxide or to benzaldehyde (arising from further oxidation of the former) is difficult to control in terms of product yield [26–31,40,45]. This can be challenging when aiming at a specific product, resulting in increased costs and waste due to both the inefficiency of the process and product separation procedures. Recently, there has been evidence for the addition of additives that could prevent further oxidation of reaction products and control selectivity [47]. This demonstrates how an adequate choice of solvent could modulate product yield, especially in the case were sensitive reaction products are obtained, such as styrene oxide.

4. Conclusions

In this work, we described the differences observed when a given epoxidation reaction is conducted in different solvents. The most striking effect concerns the reaction kinetics, which is largely sensitive to the solvent change. From our research, it can be assumed that the hydrogen bond capabilities of a given solvent are relevant enough to support the observed phenomena. This is true when the solvent is acetonitrile—H-bonding yielding slower kinetics, or toluene—non-H-bonding yielding faster kinetics without major effects on product selectivity at isoconversion for most cases. There was an exception—styrene oxidation, whose kinetics and product selectivity were both found to be affected by the solvent. In this case, it is known that styrene oxide can yield benzaldehyde by over-oxidation. In the present case, we observed that when the H-bonding solvent was used, a much lower amount of benzaldehyde was obtained when compared with when the non-H-bonding solvent was used instead. We also extended the concept to confirm a mechanistic proposal on the acid-catalyzed transformation of styrene epoxide into benzaldehyde, which was successfully demonstrated and confirmed via the stabilizing effect of an H-bonding solvent in controlling product selectivity.

In summary, this work provides evidence on the specific role of solvents in contributing to the control of reactions (kinetics and product selectivity) while agreeing with other literature reports under the same scope. Moreover, we also envisage that using protic solvents will results in stronger hindrance or modulation effects due to the fact that such class of solvents can establish strong hydrogen bonds. We are currently addressing this issue in our lab and hope to confirm this theory in the medium term.

Supplementary Materials: The following are available online at https://www.mdpi.com/article/10.3390/chemistry3030054/s1: Detailed experimental and computational procedures. Table S1—Isotope substitution scheme used in neutron experiments. Figure S1—XRD powder patterns of MCM_C and MCM_{AW} materials. Table S2—Results of catalytic experiments. Figure S2—Oxidation products detected for the reactions carried out in this study. Coordinates of the optimized geometries for the calculated species represented in Figure 5 and the isolated monomers (styrene oxide, toluene, and acetonitrile).

Author Contributions: R.N.S.: investigation, formal analysis, and writing—original draft. S.K.C.: conceptualization, investigation, formal analysis, data curation, and writing—review and editing. P.D.V.: conceptualization, investigation, data curation, formal analysis, and writing—review and editing. C.D.N.: conceptualization, methodology, supervision, project administration, formal analysis,

and writing—review and editing. All authors have read and agreed to the published version of the manuscript.

Funding: Fundação para a Ciência e Tecnologia (FCT), Portugal funded this research and is acknowledged for financial support through grants UIDB/00100/2020 and UIDP/00100/2020.

Data Availability Statement: Data from the neutron scattering experiments can be accessed freely at https://doi.org/10.5286/ISIS.E.RB1600022 (accessed on 18 June 2021).

Acknowledgments: Experiments at the ISIS Neutron and Muon Source were supported by a beamtime allocation RB1600022 from the Science and Technology Facilities Council [48]. G09 calculations were made possible due to the computing resources provided by STFC Scientific Computing Department's SCARF cluster.

Conflicts of Interest: All authors declare no conflict of interest.

References

1. Zaccaria, F.; Fagiolari, L.; Macchioni, A. Optimizing noble metals exploitation in water oxidation catalysis by their incorporation in layered double hydroxides. *Inorg. Chim. Acta* **2021**, *516*, 120161. [CrossRef]
2. Goyal, R.; Singh, O.; Agrawal, A.; Samanta, C.; Sarkar, B. Advantages and limitations of catalytic oxidation with hydrogen peroxide: From bulk chemicals to lab scale process. *Catal. Rev.* **2020**, 1–57. [CrossRef]
3. Nasrollahzadeh, M.; Sajjadi, M.; Shokouhimehr, M.; Varma, R.S. Recent developments in palladium (nano)catalysts supported on polymers for selective and sustainable oxidation processes. *Coord. Chem. Rev.* **2019**, *397*, 54–75. [CrossRef]
4. Ahn, S.; Hong, M.; Sundararajan, M.; Ess, D.H.; Baik, M.H. Design and Optimization of Catalysts Based on Mechanistic Insights Derived from Quantum Chemical Reaction Modeling. *Chem. Rev.* **2019**, *119*, 6509–6560. [CrossRef]
5. Vedrine, J.C. Metal Oxides in Heterogeneous Oxidation Catalysis: State of the Art and Challenges for a More Sustainable World. *ChemSusChem* **2019**, *12*, 577–588. [CrossRef]
6. Vedrine, J.C. Heterogeneous Catalysis on Metal Oxides. *Catalysts* **2017**, *7*, 341. [CrossRef]
7. Clarke, C.J.; Tu, W.-C.; Levers, O.; Bröhl, A.; Hallett, J.P. Green and Sustainable Solvents in Chemical Processes. *Chem. Rev.* **2018**, *118*, 747–800. [CrossRef]
8. Kajbafvala, A.; Ali, M.E.; Rahman, M.M.; Sarkar, S.M.; Hamid, S.B.A. Heterogeneous Metal Catalysts for Oxidation Reactions. *J. Nanomater.* **2014**, 1687–4110. [CrossRef]
9. Leus, K.; Liu, Y.-Y.; Van Der Voort, P. Metal-Organic Frameworks as Selective or Chiral Oxidation Catalysts. *Catal. Rev.* **2014**, *56*, 1–56. [CrossRef]
10. Valange, S.; Vedrine, J.C. General and Prospective Views on Oxidation Reactions in Heterogeneous Catalysis. *Catalysts* **2018**, *8*, 483. [CrossRef]
11. Kholdeeva, O.; Maksimchuk, N. Metal-Organic Frameworks in Oxidation Catalysis with Hydrogen Peroxide. *Catalysts* **2021**, *11*, 283. [CrossRef]
12. Trehoux, A.; Guillot, R.; Clemancey, M.; Blondin, G.; Latour, J.M.; Mahy, J.P.; Avenier, F. Bioinspired symmetrical and unsymmetrical diiron complexes for selective oxidation catalysis with hydrogen peroxide. *Dalton Trans.* **2020**, *49*, 16657–16661. [CrossRef]
13. Wang, S.; Liu, Y.; Zhang, Z.; Li, X.; Tian, H.; Yan, T.; Zhang, X.; Liu, S.; Sun, X.; Xu, L.; et al. One-Step Template-Free Fabrication of Ultrathin Mixed-Valence Polyoxovanadate-Incorporated Metal Organic Framework Nanosheets for Highly Efficient Selective Oxidation Catalysis in Air. *ACS Appl. Mater. Interf.* **2019**, *11*, 12786–12796. [CrossRef]
14. Kholdeeva, O.A. Liquid-phase selective oxidation catalysis with metal-organic frameworks. *Catal. Today* **2016**, *278*, 22–29. [CrossRef]
15. Guo, Z.; Liu, B.; Zhang, Q.H.; Deng, W.P.; Wang, Y.; Yang, Y.H. Recent advances in heterogeneous selective oxidation catalysis for sustainable chemistry. *Chem. Soc. Rev.* **2014**, *43*, 3480–3524. [CrossRef]
16. Boisvert, L.; Goldberg, K.I. Reactions of Late Transition Metal Complexes with Molecular Oxygen. *Acc. Chem. Res.* **2012**, *45*, 899–910. [CrossRef]
17. Hermans, I.; Spier, E.S.; Neuenschwander, U.; Turra, N.; Baiker, A. Selective Oxidation Catalysis: Opportunities and Challenges. *Top. Catal.* **2009**, *52*, 1162–1174. [CrossRef]
18. Fernandes, C.I.; Vaz, P.D.; Nunes, T.G.; Nunes, C.D. Zinc biomimetic catalysts for epoxidation of olefins with H_2O_2. *Appl. Clay Sci.* **2020**, *190*, 105562. [CrossRef]
19. Fernandes, C.I.; Vaz, P.D.; Nunes, C.D. Selective and Efficient Olefin Epoxidation by Robust Magnetic Mo Nanocatalysts. *Catalysts* **2021**, *11*, 380. [CrossRef]
20. Zhang, L.L.; Zhang, Z.Y.; He, X.P.; Zhang, F.; Zhang, Z.B. Regulation of the products of styrene oxidation. *Chem. Eng. Res. Des.* **2017**, *120*, 171–178. [CrossRef]
21. Sun, W.L.; Hu, J.L. Oxidation of styrene to benzaldehyde with hydrogen peroxide in the presence of catalysts obtained by the immobilization of $H_3PW_{12}O_{40}$ on SBA-15mesoporous material. *React. Kinet. Mech. Catal.* **2016**, *119*, 305–318. [CrossRef]

22. Fu, Y.H.; Xu, L.; Shen, H.M.; Yang, H.; Zhang, F.M.; Zhu, W.D.; Fan, M.H. Tunable catalytic properties of multi-metal-organic frameworks for aerobic styrene oxidation. *Chem. Eng. J.* **2016**, *299*, 135–141. [CrossRef]
23. Neto, A.D.S.; Pinheiro, L.G.; Filho, J.M.; Oliveira, A.C. Studies on styrene selective oxidation over iron-based catalysts: Reaction parameters effects. *Fuel* **2015**, *150*, 305–317. [CrossRef]
24. Wang, Q.; Zhang, Y.; Yu, L.; Yang, H.; Mahmood, M.H.R.; Liu, H.Y. Solvent effects on the catalytic activity of manganese(III) corroles. *J. Porphyr. Phthalocyanines* **2014**, *18*, 316–325. [CrossRef]
25. Saux, C.; Pierella, L.B. Studies on styrene selective oxidation to benzaldehyde catalyzed by Cr-ZSM-5: Reaction parameters effects and kinetics. *Appl. Catal. A-Gen.* **2011**, *400*, 117–121. [CrossRef]
26. Fernandes, C.I.; Rudić, S.; Vaz, P.D.; Nunes, C.D. Looking inside the pores of a MCM-41 based Mo heterogeneous styrene oxidation catalyst: An inelastic neutron scattering study. *Phys. Chem. Chem. Phys.* **2016**, *18*, 17272–17280. [CrossRef]
27. Bento, A.; Sanches, A.; Vaz, P.D.; Nunes, C.D. Catalytic Application of Fe-doped MoO_2 Tremella-Like Nanosheets. *Top. Catal.* **2016**, *59*, 1123–1131. [CrossRef]
28. Pan, Z.; Hua, L.; Qiao, Y.; Yang, H.; Zhao, X.; Feng, B.; Zhu, W.; Hou, Z. Nanostructured Maghemite-Supported Silver Catalysts for Styrene Epoxidation. *Chin. J. Catal.* **2011**, *32*, 428–435. [CrossRef]
29. Huang, C.; Zhang, H.; Sun, Z.; Zhao, Y.; Chen, S.; Tao, R.; Liu, Z. Porous Fe_3O_4 nanoparticles: Synthesis and application in catalyzing epoxidation of styrene. *J. Colloid Interf. Sci.* **2011**, *364*, 298–303. [CrossRef]
30. Guin, D.; Baruwati, B.; Manorama, S.V. A simple chemical synthesis of nanocrystalline AFe_2O_4 (A = Fe, Ni, Zn): An efficient catalyst for selective oxidation of styrene. *J. Mol. Catal A Chem.* **2005**, *242*, 26–31. [CrossRef]
31. Tong, J.; Cai, X.; Wang, H.; Zhang, Q. Improvement of catalytic activity in selective oxidation of styrene with H_2O_2 over spinel Mg–Cu ferrite hollow spheres in water. *Mater. Res. Bull.* **2014**, *55*, 205–211. [CrossRef]
32. Corma, A.; Esteve, P.; Martínez, A. Solvent Effects during the Oxidation of Olefins and Alcohols with Hydrogen Peroxide on Ti-Beta Catalyst: The Influence of the Hydrophilicity–Hydrophobicity of the Zeolite. *J. Catal.* **1996**, *161*, 11–19. [CrossRef]
33. Batra, M.S.; Dwivedi, R.; Prasad, R. Recent Developments in Heterogeneous Catalyzed Epoxidation of Styrene to Styrene Oxide. *Chem. Select* **2019**, *4*, 11636–11673. [CrossRef]
34. Chen, H.; Wang, W.; Yang, Y.; Jiang, P.; Gao, W.; Cong, R.; Yang, T. Solvent effect on the formation of active free radicals from H_2O_2 catalyzed by Cr-substituted PKU-1 aluminoborate: Spectroscopic investigation and reaction mechanism. *Appl. Cala A Gen.* **2019**, *588*, 117283. [CrossRef]
35. Shen, Y.; Jiang, P.; Wai, P.T.; Gu, Q.; Zhang, W. Recent Progress in Application of Molybdenum-Based Catalysts for Epoxidation of Alkenes. *Catalysts* **2019**, *9*, 31. [CrossRef]
36. Emenike, B.U.; Spinelle, R.A.; Rosario, A.; Shinn, D.W.; Yoo, B. Solvent Modulation of Aromatic Substituent Effects in Molecular Balances Controlled by CH-pi Interactions. *J. Phys. Chem. A* **2018**, *122*, 909–915. [CrossRef]
37. Fraile, J.M.; Garcia, N.; Mayoral, J.A.; Santomauro, F.G.; Guidotti, M. Multifunctional Catalysis Promoted by Solvent Effects: Ti-MCM41 for a One-Pot, Four-Step, Epoxidation-Rearrangement-Oxidation-Decarboxylation Reaction Sequence on Stilbenes and Styrenes. *ACS Catal.* **2015**, *5*, 3552–3561. [CrossRef]
38. Koohestani, B.; Ahmad, A.L.; Bhatia, S.; Ooi, B.S. Vanadium Oxide-Based Composite Catalysts for the Oxidation of Styrene: A Comparative Study. *Curr. Nanosci.* **2011**, *7*, 781–789. [CrossRef]
39. Szala-Bilnik, J.; Falkowska, M.; Bowron, D.T.; Hardacre, C.; Youngs, T.G.A. The Structure of Ethylbenzene, Styrene and Phenylacetylene Determined by Total Neutron Scattering. *ChemPhysChem* **2017**, *18*, 2541–2548. [CrossRef]
40. Fernandes, C.I.; Saraiva, M.S.; Nunes, T.G.; Vaz, P.D.; Nunes, C.D. Highly enantioselective olefin epoxidation controlled by helical confined environments. *J. Catal.* **2014**, *309*, 21–32. [CrossRef]
41. Zheng, Y.-Z.; Wang, N.-N.; Luo, J.-J.; Zhou, Y.; Yu, Z.-W. Hydrogen-bonding interactions between [BMIM][BF4] and acetonitrile. *Phys. Chem. Chem. Phys.* **2013**, *15*, 18055–18064. [CrossRef]
42. Platt, S.P.; Attah, I.K.; El-Shall, M.S.; Hilal, R.; Elroby, S.A.; Aziz, S.G. Unconventional $CH^{\delta+}\cdots N$ hydrogen bonding interactions in the stepwise solvation of the naphthalene radical cation by hydrogen cyanide and acetonitrile molecules. *Phys. Chem. Chem. Phys.* **2016**, *18*, 2580–2590. [CrossRef] [PubMed]
43. Youngs, T.G.A.; Manyar, H.; Bowron, D.T.; Gladden, L.F.; Hardacre, C. Probing chemistry and kinetics of reactions in heterogeneous catalysts. *Chem. Sci.* **2013**, *4*, 3484–3489. [CrossRef]
44. Silva, N.U.; Fernandes, C.I.; Nunes, T.G.; Saraiva, M.S.; Nunes, C.D.; Vaz, P.D. Performance evaluation of mesoporous host materials in olefin epoxidation using Mo(II) and Mo(VI) active species-Inorganic vs. hybrid matrix. *Appl. Catal. A Gen.* **2011**, *408*, 105–116. [CrossRef]
45. Fernandes, C.I.; Stenning, G.B.G.; Taylor, J.D.; Nunes, C.D.; Vaz, P.D. Helical Channel Mesoporous Materials with Embedded Magnetic Iron Nanoparticles: Chiral Recognition and Implications in Asymmetric Olefin Epoxidation. *Adv. Synth. Catal.* **2015**, *357*, 3127–3140. [CrossRef]
46. Nunes, C.D.; Rudić, S.; Vaz, P.D. Probing the Relevance of MoO_2 Nanoparticle Synthesis in Their Catalytic Activity by Inelastic Neutron Scattering. *Phys. Chem. Chem. Phys.* **2020**, *22*, 896–904. [CrossRef] [PubMed]
47. Sankar, M.; Nowicka, E.; Carter, E.; Murphy, D.M.; Knight, D.W.; Bethell, D.; Hutchings, G.J. The benzaldehyde oxidation paradox explained by the interception of peroxy radical by benzyl alcohol. *Nature Comm.* **2014**, *5*, 3332. [CrossRef]
48. Vaz, P.D.; Nunes, C.D.; Callear, S. *The Active Role of Solvents in Oxidation Catalysis*; STFC ISIS Facility: UK, 2015. [CrossRef]